SCANNING VOL. 25, 257–263 (2003)

Received: October 23, 2002
Accepted with revision: June 11, 2003

Three-Dimensional Architecture of Ribosomal DNA within Barley Nucleoli Revealed with Electron Microscopy

MEGUMI IWANO, FANG-SIK CHE, SEIJI TAKAYAMA, KIICHI FUKUI,* AKIRA ISOGAI

Graduate School of Biological Sciences, Nara Institute of Science and Technology, Nara; *Department of Biotechnology, Graduate School of Engineering, Osaka University, Suita, Japan

Summary: To elucidate the topological positioning of ribosomal RNA genes (rDNA) and nucleolar structure in three dimensions, we examined the localization of rDNA using in situ hybridization (ISH) analysis by scanning electron microscopy (SEM). The rDNA genes within the three-dimensional architecture of nucleoli were detected on chromatin fibers that connect a thick strand-like structure and a protrusion of rDNA into the inner nuclear hole where the nucleolus is formed. This novel use of ISH together with SEM is useful for the analysis of nucleolar structure in detail. Furthermore, rDNA was detected at the periphery of the fibrillar centers (FCs) of the nucleolus using immunogold labeling together with transmission electron microscopy (TEM). In situ hybridization with TEM confirmed that rDNA is naked and thus active in the FCs of nucleoli; ISH with SEM confirmed that rDNA is not covered with ribonucleo proteins at the protruding point and is thus inactive. We also show that the distribution pattern of FCs differs from sample to sample. These results indicate that rDNA is transcribed dynamically in a time- and region-specific manner over the course of the cell cycle.

Key words: barley, in situ hybridization (ISH), nucleoli, ribosomal DNA, scanning electron microscopy

PACS: 61.16.Bg, 87.64.Dz

Introduction

Nucleoli, the sites of ribosome biogenesis, are meticulously organized subnuclear organelles (Goessens 1984, Scheer and Rose 1984). During ribosome biogenesis, nucleoli are involved in the transcription of ribosomal RNA genes (rDNA). Multiple steps are required for the proper maturation of the preribosomal subunit, including the processing of pre-ribosomal RNA and the association of ribosomal proteins (Brown and Shaw 1998, Hozak *et al.* 1994, Shaw and Jordan 1995). Observation by transmission electron microscopy (TEM) in both animals (Goessens 1984, Jordan and McGovern 1981, Wachtler and Stahl 1993) and plants (Risueno *et al.* 1982, Sato 1992) has revealed that the nucleolus possesses different structural components: fibrillar centers (FCs), a dense fibrillar component (DFC), and a granular component (GC) (Jordan 1984).

To clarify the relationship between these structural findings and the transcription of rDNA, immunological analysis on the distribution of RNA polymerase I (Scheer and Rose 1984) and DNA (Charest *et al.* 1985, Martin and Medina 1992), as well as in situ hybridization (ISH) analysis using rDNA probes for the nucleolus, were performed (Leitch *et al.* 1992, Thiry and Thiry-Blaise 1989). RNA polymerase I and rDNA coexist in FCs, clearly indicating that transcription occurs in the peripheral region of FCs. On the other hand, Stahl *et al.* (1991) and Jimenez-Garcia *et al.* (1993) demonstrated the localization of rDNA in DFC and claimed that the transcription of rDNA occurs there. The function of FCs and DFC within nucleoli thus remains controversial.

The transcription and processing sites within a nucleolus were determined by a detailed positional analysis of a spacer region in both immature and mature rRNA (Bassy *et al.* 2000, Leader *et al.* 1997). In addition, localization of transcriptional factors (Martin and Medina 1992) and bromo-UTP (BrUTP) incorporation (De Carcer and Medina 1999, Yano and Sato 2000) were examined by TEM and confocal microscopy, respectively. Recent evidence suggests that transcription of rDNA and early processing of rRNA occur in the transition area between FCs and DFC (De Carcer and Medina 1999, Yano and Sato 2000). The topological localization of rDNA and/or rRNA within the nucleolus is still obscure, despite previous TEM studies that have elucidated the three-dimensional (3-D) architecture of the nucleolus (Sato 1992, Sato and Myoraku 1994, Shaw *et al.* 1995).

Address for reprints:

Megumi Iwano
Graduate School of Biological Sciences
Nara Institute of Science and Technology
Nara 630-0101
Japan
e-mail: m-iwano@bs.aist-nara.ac.jp

Scanning electron microscopy has been used frequently to observe nuclear and chromosomal structures (Iwano *et al.* 1997). A combination of physical gene localization and visualization of nucleolar structure with SEM allows a detailed analysis of the 3-D relationship between rDNA and the nucleolus. The present study reveals the 3-D architecture of the nucleolus and the localization of rDNA detected with ISH by means of SEM. Furthermore, rDNA was localized to specific regions within the nucleolus using immunostaining for DNA and ISH with an rDNA probe and imaging with TEM.

Materials and Methods

The root tips of *Hordeum vulgare*, cv. Minorimugi, were used throughout the following experiments. For ISH, a rice 45S rDNA probe was used. The 3.8-kb probe includes most of the coding regions of the three ribosomal RNA genes (18S-5.8S-26S rDNA) and the flanking spacer regions (Sano and Sano 1990) conjugated with biotin by the random-primed DNA labeling method (Nippon Gene, Tokyo, Japan). The hybridization mixture consisted of 50% formamide, 10% dextran sulfate (MW 50,000), 0.1% sodiumdodecylsulfate, 2 × SSC, the labeled probe, and salmon sperm DNA (Leitch *et al.* 1992).

For observation by TEM, root tips were fixed in a mixture of 2% paraformaldehyde and 1% glutaraldehyde. Samples were dehydrated in an ethanol series ranging from 25 to 100% and then embedded in LR white (London Resin Co., Berkshire, England) (Suzaki and Kataoka 1992). Ultra-thin sections 80 nm thick were mounted on uncoated gold grids.

For immunological detection of DNA, samples were incubated with anti-DNA mouse monoclonal IgM (Progen) followed by incubation with either 5 or 10 nm gold-conjugated anti-mouse IgM (Biocell Research Laboratories, Rancho Dominguez, Calif., USA). As a control, the primary antibody was replaced with mouse IgG or omitted from the incubation medium.

In situ hybridization was performed as described by Iwano *et al.* (2000) with the addition of a pretreatment with proteinase K (1 mg/ml) at 37°C for 20 min and a subsequent incubation in RNase A (3 mg/ml) at 37°C for 1 h. Following washing with 2 × SSC, samples were mounted on a glass slide. The hybridization mixture was layered onto the grids and covered with a coverslip at 37°C. After denaturation at 80°C for 5 min, the samples were hybridized with the rDNA probe overnight. Following stringent washing at 55°C, samples were incubated with antibiotin IgG conjugated with 15 nm gold particles. Samples were then stained with 2% uranyl acetate for 10 min. As a cytochemical control, the rDNA probe was omitted from the incubation medium. Photographs were taken under a bright field with TEM (H-7100, Hitachi, Tokyo, Japan) at an accelerating voltage of 75 keV and a beam current of 10 mA.

For ISH with SEM, samples were prepared as described previously (Iwano *et al.* 1997). Briefly, root tips were fixed with ethanol-acetic acid (3:1) and macerated using an enzyme cocktail (Fukui 1996). The root tip was placed on a microscope slide with a drop of 45% acetic acid and warmed on a hot plate. After the root tip had been squashed under a coverslip, cytoplasm was removed by addition of 45% acetic acid. Each slide was observed under a phase contrast microscope, and samples from which all the cell walls and cytoplasm had been removed, and in which the nuclei and chromosomes were well preserved, were selected for SEM. The samples were frozen in liquid nitrogen and the coverslip was removed from the sample. The samples were postfixed with a 1% glutaraldehyde solution and dehydrated through a graded ethanol series (50–100%). The samples were then critical-point dried using liquid CO_2 as a transitional fluid. After pretreatment with RNase A (3 mg/ml) at 37°C for 1 h, the samples were washed with 2 × SSC. The hybridization mixture was layered on a glass slide, covered with a coverslip, denatured at 80°C for 5 min, and subjected to overnight hybridization. After stringent washing at 55°C, the samples were incubated with an antibiotin antibody conjugated with 15 nm gold particles. As a control, the probe was omitted from the hybridization medium for some samples. Finally, the samples were postfixed in 1% OsO_4 and critical-point dried. The samples were coated with 3–5 nm of platinum/palladium (E5150, Polaron). The samples were observed using a field emission scanning electron microscope (FESEM) (4700S, Hitachi, Tokyo, Japan). Secondary electron images were captured using two secondary electron detectors placed above the objective lens (upper detector) and below the objective lens (lower detector) at 15 keV, with which we could observe the precise structure of nucleus (Sato *et al.* 1994). Backscattered electron images were taken using a yttriam aluminium garnet (YAG) backscattered electron detector at 15 keV, with which we could easily differentiate gold particles from nuclear structure.

Results and Discussion

We first examined the 3-D architecture of a nucleolus using SEM. The nucleolus is easily recognized upon phase contrast microscopy as a circular and highly refractive suborganelle of the nucleus. The nucleolus was also distinguished from the nucleoplasm as a circular structure under TEM. In this study, however, the structure of the nucleolus was completely different from what has previously been observed. The nucleolus did not show a circular or round profile, but rather appeared as a thick strand-like structure, twisted or folded into an irregular form (white arrows in Fig. 1a). The appearance was commonly observed in SEM-ISH samples. Furthermore, the surface of the nucleolus was not filamentous but rugged, and was quite different from that of the nucleoplasm, with its filamentous appearance (Fig. 1b). This result suggests that the nucleolar structure is built up by the aggregation of ribonucleo-

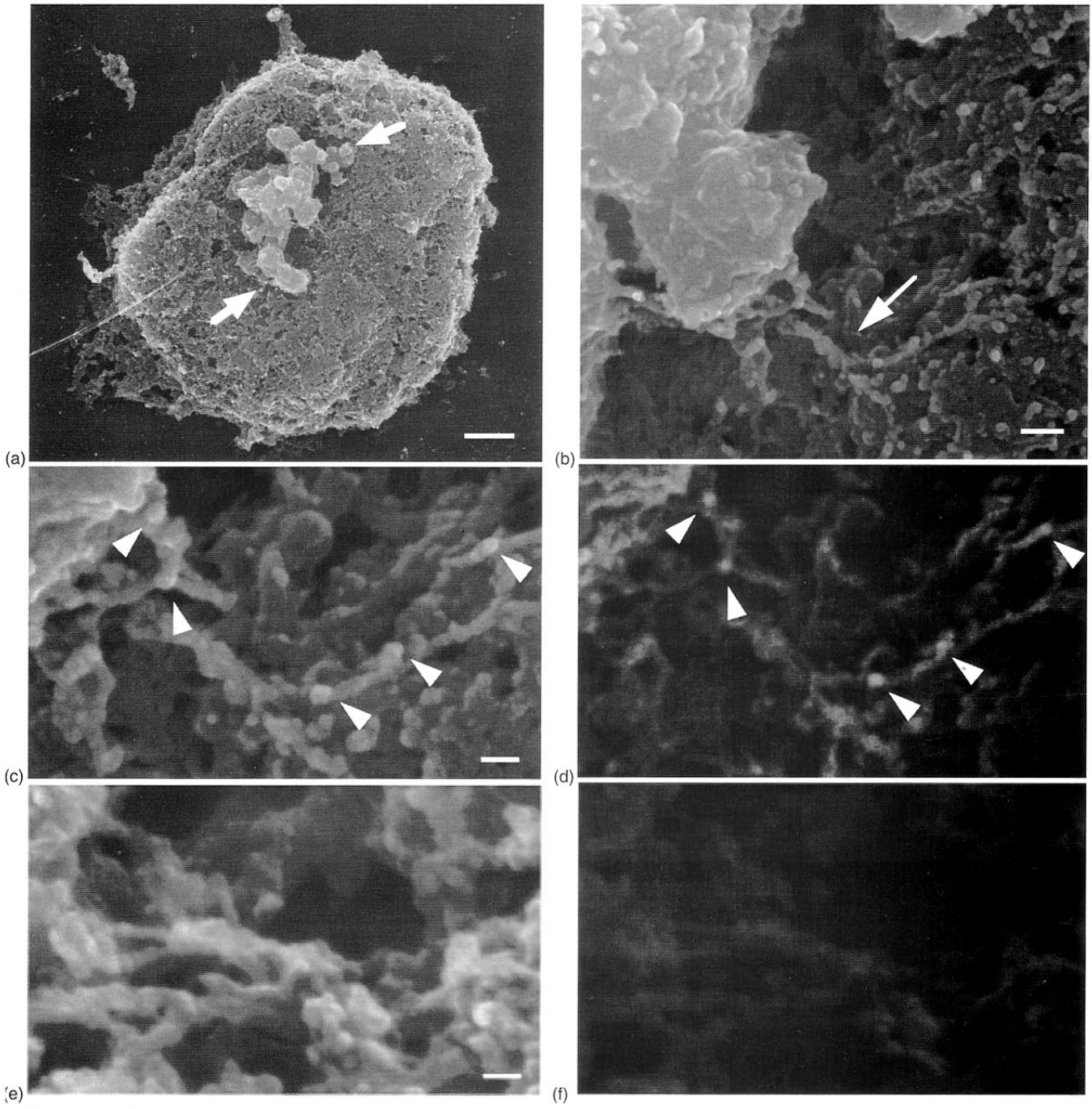

FIG. 1 Localization of rDNA detected by in situ hybridization by scanning electron microscopy. (a) A nucleus was exposed during sample preparation. The nucleolus (arrows) was observed as a thick strand-like structure. Secondary electron image. Bar = 1 μm. (b) A higher magnification of (a). An arrow shows a chromatin fiber approximately 30 nm in diameter, connecting the thick strand-like nucleolus to the inner surface of a nuclear hole. Filamentous structures of the nucleoplasm were also observed. Secondary electron image. Bar = 0.1 μm. (c) A higher magnification of the region indicated by the arrow in (b). Gold particles were observed on the fibers (arrowheads). Secondary electron image. Bar = 50 nm. (d) Backscattered electron image of the same region as in Figure (c) Arrowheads show gold particles on the chromatin fiber. (e) A higher magnification of chromatin fibers in a control nucleus. There were no gold particles. Secondary electron image. Bar = 50 nm. (f) Backscattered electron image of the same region as in (e).

proteins (RNPs) onto rDNA strands, which are transcriptional products upon which ribosomes are formed. In the connection region between the thick strand-like nucleolus and the inner surface of a nuclear hole, RNPs were not observed; instead, ordinary and naked chromatin fibers about 30 nm in diameter (an arrow in Fig. 1b and c) were seen. On the chromatin fibers, some particles on the chromatin fibers in the secondary electron image (arrowheads in Fig.

1c) were identified as gold particles by the backscattered electron image (arrowheads in Fig. 1d). On the other hand, when the probe was omitted from the hybridization mixture as a negative control, there were no gold particles on the chromatin fibers in the backscattered electron image (Fig. 1e and f). The fact that the naked chromatin fiber in the connection region (an arrow in Fig. 1b) is rDNA indicates the lack of rRNA transcription in this region.

During sample preparation, most nucleoli were removed from nuclei, forming concave depressions in the nuclei (arrows in Fig. 2a). As a result, the rDNA in the connection region between the nucleoplasm and the extracted thick strand-like nucleolus was clearly observed with SEM (Fig. 2b and c). Both images obtained through the capturing of secondary electrons (Fig. 2b) and backscattering electrons (Fig. 2c) indicated the localization of gold particles in these protruding connection regions (arrowhead in Fig. 2a). Comparison between these two images indicated that the backscattered image provided a clearer visualization of clusters of gold particles on the surface of the protruding rDNA region and into the inner nuclear hole formed by the removal of the thick strand-like nucleolar structure (Fig. 1).

Furthermore, we examined the localization of DNA in nuclear cross sections by immunogold labeling using TEM. Gold particles accumulated on the condensed chromatin in the nucleoplasm, as shown by arrowheads in Figure 3a. Because the samples prepared for this study were fixed in a mixture of 2% paraformaldehyde and 1% glutaraldehyde, without osmium fixation, FCs in the nucleolus appeared as electron-translucent patches (arrows in Fig. 3a). Dense fibrillar component and the GC (Jordan 1984) were observed as relatively electron-dense and uniform regions, which occupied most of the nucleolus under these fixation conditions. Within the nucleolus, gold particles were observed at the peripheral regions of the FCs (Fig. 3a), but never in the DFC and GC. When the primary antibody was replaced with mouse IgG as a negative control, no gold particles were observed in the nucleolus (Fig. 3b).

We then examined the localization of rDNA by ISH with TEM. In nuclear cross sections, we observed a cluster of gold particles on the condensed chromatin in the outer perinucleolar regions, which is referred as the nucleolar-associated chromatin (NAC) (Jordan 1984) (arrowhead in Fig. 3c). This region corresponds to the outer portion of the nucleolar organization region (NOR), where the tandem arrays of rDNA sequences exist. A cluster of gold particles was also observed in the NAC region, which protruded from the nucleoplasm into the nucleolus as shown by an arrowhead in Figure 3d. In this region, gold particles are lined up on a face of the invaginated area of the nucleolus. Within the nucleolus, gold particles were observed at the inner periphery of the FCs (arrows in Fig. 3d and e). The results indicate that the rDNA in the FCs is not associated with RNPs that are located at the surroundings of the outer regions of FCs (De Carcer and Medina 1999). When the rDNA probe was omitted from the hybridization mixture as a negative control, no gold particles were observed in the

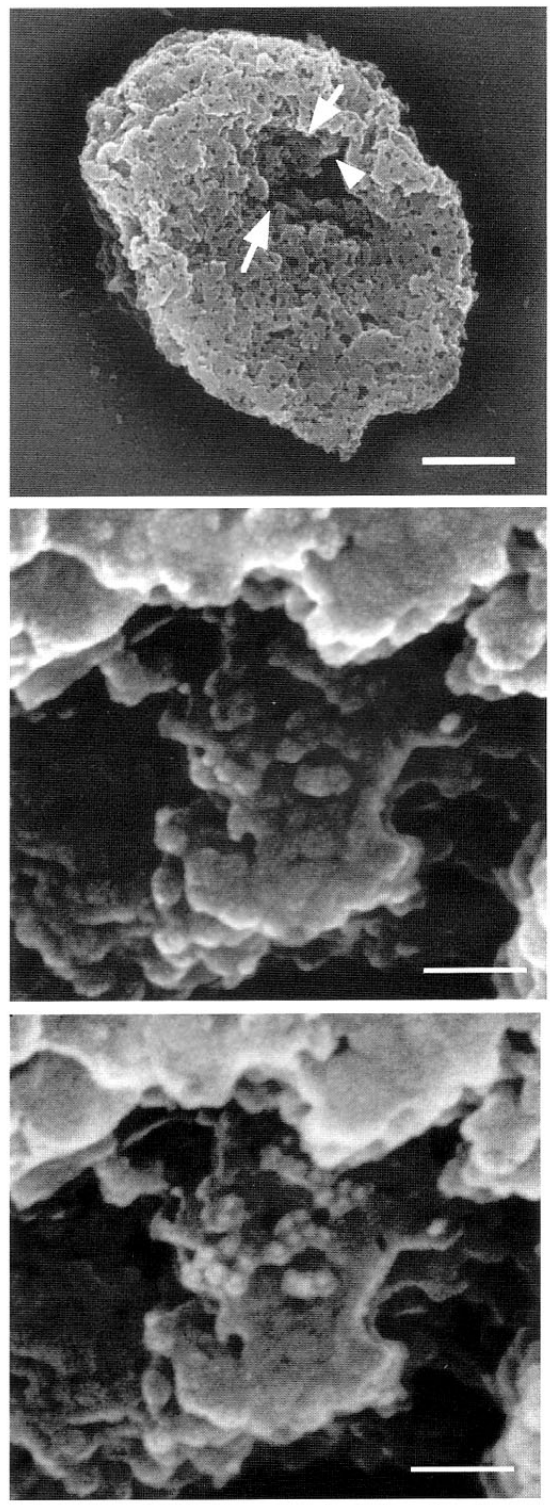

FIG. 2 Localization of rDNA detected by in situ hybridization with scanning electron microscopy. (a) A nucleolus was removed from the nucleus during sample preparation. Arrows indicate a nuclear hole formed by nucleolar removal. An arrowhead indicates the protruding connection region to a previously extracted nucleolus. Secondary electron image. Bar = 1 μm. (b) A higher-magnification, secondary-electron image of the region indicated by the arrow in (a). Bar = 0.1 μm. (c) Backscattered electron image of the same region as in (b). In the protruding rDNA, clusters of gold particles were observed. Bar = 0.1 μm.

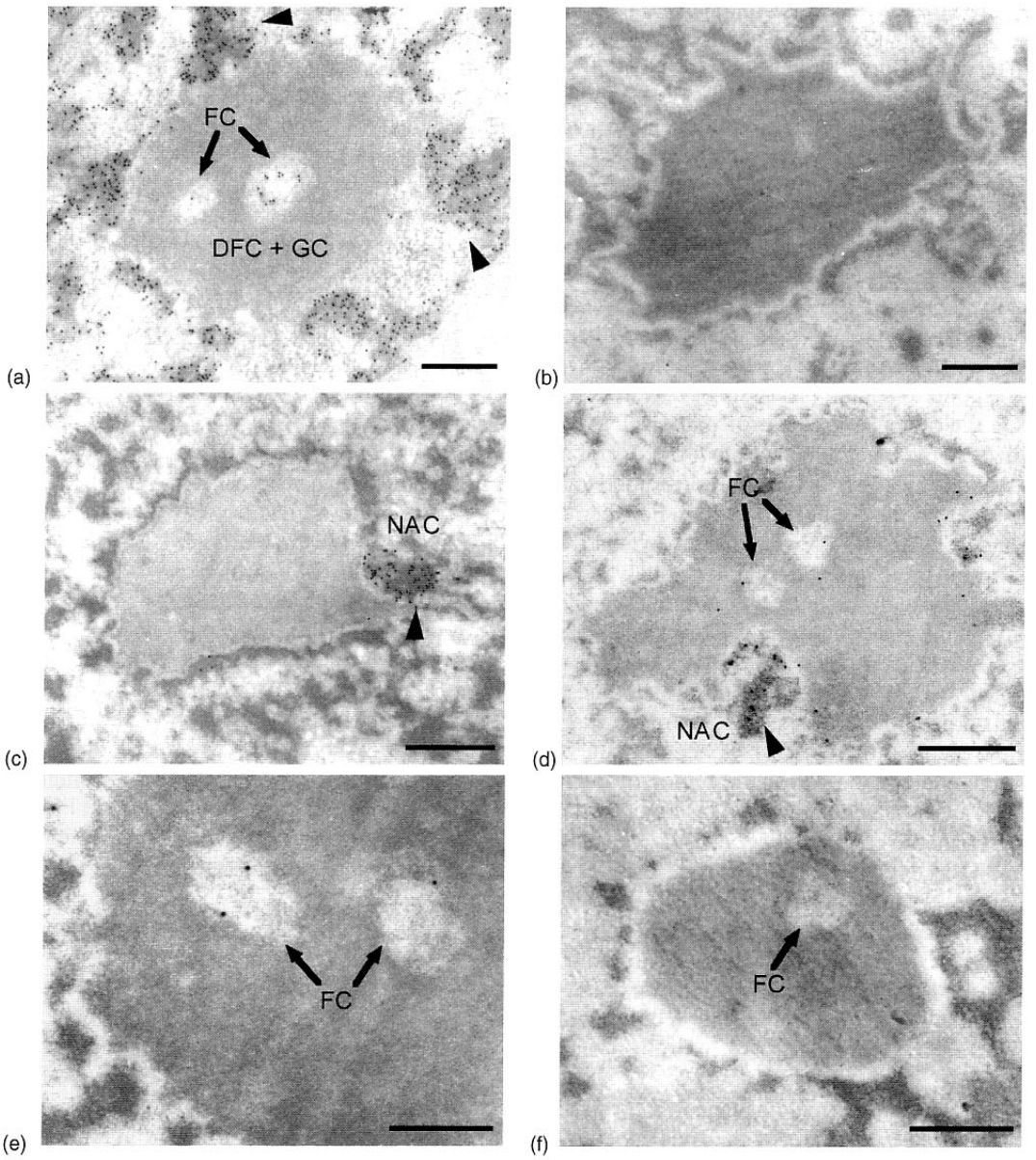

FIG. 3 Examination of a barley nucleus with immunogold staining and in situ hybridization (ISH) using an rDNA probe. (a) Localization of rDNA in a barley nucleus by immunogold staining. Within the nucleolus, gold particles were detected in the inner periphery of the fibrillar centers (FCs), which appear as electron translucent areas. Arrows indicate FCs. Arrowheads indicate the condensed chromatin in the nucleoplasm. Dense fibrillar and granular components (DFC and GC) were observed as a relatively electron-dense region. Bar = 0.5 μm. (b) A nucleolus in a negative control of immunogold staining, in which the primary antibody was replaced with mouse IgG. Bar = 0.5 μm. (c) In situ hybridization (ISH) with transmission electron microscopy (TEM). Gold particles were observed as a cluster in the nucleolar-associated chromatin (NAC) and are shown by an arrowhead. Gold particles were not observed in DFC and GC. Bar = 0.5 μm. (d) In situ hybridization with TEM. The NAC protruded from the nucleoplasm to nucleolus and is shown by an arrowhead. A cluster of gold particles was observed in the protruding NAC. Within the nucleolus, gold particles were observed in the FCs. Bar = 0.5 μm. (e) In situ hybridization with TEM. Gold particles were observed in electron-translucent FCs (arrows) using TEM. Bar = 0.2 μm. (f) A nucleolus in a negative control of ISH with TEM. Bar = 0.5 μm.

nucleolus (Fig. 3f). It is known that intranucleolar chromatin stained with osmium amine-B forms a complex filamentous structure, and that this clump of chromatin coexists with fibrillar chromatin in maize nucleoli (Motte *et al.* 1991). This pattern has been also observed in wheat nucleoli by fluorescence in situ hybridization (FISH) analysis (Leitch *et al.* 1992). The distribution pattern of gold particles revealed by this study (Fig. 3c, d, and e) strongly indicates that barley rDNA forms a clumped, but loose structure in the nucleolus. Some models have been proposed for the functional organization of rDNA in the nucleolus (Brown and Shaw 1998, De Carcer and Medina 1999). These models propose that rDNA at the periphery of FCs and/or transitional regions of FCs to DFC, such as that la-

beled in Figure 3d and e, is transcriptionally active. This conclusion is consistent with the previous models presented by Thiry and Thiry-Blaise (1989).

In the cross sections, a part of NAC was observed to protrude from the nucleoplasm into the nucleolus (Fig. 3d). Because a cluster of gold particles was detected in the NAC, the region would correspond to a clump of the NOR, suggesting that the rDNA would extend from the protruded NAC to the nucleolus. In this study, the 3-D structure of this protruding NAC was also observed with SEM; namely, the chromatin fiber, which was observed at the connection region between the thick strand-like nucleolus and the inner surface of a nuclear hole (Fig. 1b), would correspond to such a protruding NAC (arrow in Fig. 3d). On the other hand, the protruding rDNA that was visualized in the inner nuclear hole formed after nucleolar extraction (Fig. 2b and c), could correspond to the protruding NAC. In the area of connection between the nucleolus and the NAC, rDNA was found to extend from the NOR chromosome and to remain relatively naked, compared with those in the thick strand-like nucleolus, which form complexes composed of RNPs, rDNA, and rRNA. In situ hybridization visualized with TEM and SEM demonstrated the existence of multiple copies of rDNA in this area, although this area was made fragile by the sample preparation for SEM. Concerning the orientation of the NOR in the peripheral region of the nucleolus, FISH analysis under confocal laser microscopy has been performed well (Leitch *et al.* 1992). Recently, high-voltage TEM has been used to examine the 3-D orientation of the NOR (Gonzalez-Melendi and Shaw 2002). It has been difficult, however, to clarify the orientation of the NOR in relation to the 3-D structure of the nucleolus. In this study, the 3-D localization of rDNA in combination with the direct observation of nucleolar structure was achieved using in situ hybridization together with SEM.

Estable (1966) proposed that the nucleolus consists of molecules organized in structures—the "nucleonema"—and molecules not organized into structures—the "pars amorpha." He also reported that the nucleonema forms a reticulum of sheets or strands and is stained by silver impregnation. By conventional analysis of serial sections using silver staining, it was shown that the nucleolus consists of 0.35 μm thick strand-like elements and a coiled-up structure about 1 μm in diameter (Sato 1992). Based on the results that DFC contains proteins with a high affinity to silver, he suggested that the strand-like structure, the nucleonema, is formed by DFC (Sato 1992). In our current study, the nucleolus showed thick strand-like structures with diameters of about 0.3–0.5 μm by SEM, suggesting that these structures represent the DFC-filled nucleonema. Furthermore, it has been reported that a nucleolus in the interphase nucleus of pancreatic acinar shows the thick strand-like structure (Cheniclet *et al.* 1995). Thus, the thick strand-like structure of a nucleolus would be a universal structure in plants and animals.

When we observe living cells using a phase-contrast microscopy, the nucleolus appears as a round and homogeneous structure. In the sample prepared for TEM and SEM, however, a nucleolus appears as a complex structure. In this study, a nucleolus showed the thick strand-like structure in the SEM-ISH sample. The sample for the SEM-ISH was fixed with acetic acid-alcohol, and then proteins in a nucleolus would not be cross linked. Furthermore, the samples were pretreated with RNase A (3 mg/ml) at 37°C for 1 h before hybridization. Therefore, it is speculated that the treatment acts on binds between proteins and RNA, or RNPs to disrupt GC complex, which consists of rRNA and proteins. As a result, only DFC and FC would be conserved as the thick strand-like structure.

De Carcer and Medina (1999) visualized the localization of abundant RNPs and transcription factors by immunohistochemistry using confocal microscopy. They also detected the transcription site by BrUTP incorporation by TEM. Transcription factors and BrUTP existed in a reticulated pattern within the DFC, which corroborates the conclusion in this study that the reticulated and thick strand-like structures correspond to the DFC components of the nucleoli. According to a model by De Carcer and Medina (1999), the peripheral region of FCs functions as a center where rDNA is actively transcribed. The proteins for transcription and transcribed RNA would aggregate around rDNA at the FCs to form DFC structures. Therefore, DFC might represent aggregates of RNAs and proteins around FCs. In this study, DFC appeared as a thick strand-like structure upon SEM, and as a homogeneous structure by TEM.

Conclusion

In this study, we demonstrated the localization of rDNA at specific regions of the nucleolus using ISH and visualizing with SEM and TEM. By SEM observation, the nucleolus appeared as a thick strand-like structure. Using ISH together with SEM, rDNA genes were detected on chromatin fibers connected to this structure. When the nucleolus was removed during the sample preparation, a cluster of rDNA genes was detected directly where the rDNA protrudes into the inner nuclear hole. Furthermore, using ISH together with TEM, rDNA was detected in FCs and in the protruding NAC. This latter site corroborates the perinucleolar localization seen in SEM. These results clearly illustrate the possibility of 3-D localization and direct visualization of rDNA by SEM. These results also prove that ISH with SEM is effective not only in the detection of genes but also in the analysis of the 3-D architecture of the nucleolus.

Acknowledgment

The authors are grateful to Nobuko Ohmido (Kobe University, Kobe, Japan) for her helpful suggestions.

References

Bassy O, Jimenez-Garcia LF, Echeverria O M, Vazquez-Nin GH, Moreno Diaz de la Espina S: High resolution detection of rRNA and rDNA in plant nucleoli with different activities by in situ hybridization. *Biol Cell* 92, 59–70 (2000)

Brown JWS, Shaw PJ: Small nucleolar RNAs and pre-rRNA processing in plants. *Plant Cell* 10, 649–657 (1998)

Charest PM, Bergergon F, Lafontaine JG: Ultrastructural localization of DNA and RNA in *Allium porrum* interphase cells by means of nuclease-gold complexes. *Histochem J* 17, 957–962 (1985)

Cheniclet C, Garzon S, Bendayan M: In situ detection of nucleic acids by the nuclease-gold method In: *Visualization of Nucleic Acids* (Ed. Morel G). CRC Press, Boca Raton, 95–109 (1995)

De Carcer G, Medina FJ: Simultaneous localization of transcription and early processing markers allows dissection of functional domains in the plant cell nucleolus. *J Struct Biol* 128, 139–151 (1999)

Estable C: Morphology, structure and dynamics of the nucleonema. *Natl Cancer Inst Monogr* 23, 91–105 (1966)

Fukui K: Mitosis. In *Plant Chromosomes.* (Eds. Fukui K, Nakayama S). *LabMeth,* CRC Press, Boca Raton, 1–18 (1996)

Goessens G: Nucleolar Structure. *Int Rev Cytol* 87, 107–158 (1984)

Gonzalez-Melendi P, Shaw P: 3D gold in situ labeling in the EM. *Plant J* 29, 237–243 (2002)

Hozak P, Cook PR, Schofer C, Mosgoller W, Wachtler F: Site of transcription of ribosomal RNA and intranucleolar structure in Hela cells. *J Cell Sci* 107, 639–648 (1994)

Iwano M, Fukui K, Takaichi S, Isogai A: Globular and fibrous structure in barley chromosomes revealed by high-resolution scanning electron microscopy. *Chromosome Res* 5, 341–349 (1997)

Iwano M, Ogasawara Y, Hase H, Nakamura H, Yokomura E, Nakajima Y, Fukui K, Isogai A: The assembly of plasmid DNA and chromatophore in *Rhodospirillum rubrum. Protoplasma.* 214, 158–165 (2000)

Jimenez-Garcia LF, Segura-Valdez ML, Ochs RL, Echeverria OM, Vazquez-Nin GH, Busch H: Electron microscopic localization of ribosomal DNA in rat liver nucleoli by nonisotopic in situ hybridization. *Exp Cell Res* 207, 220–225 (1993)

Jordan EG: Nucleolar nomenclature. *J Cell Sci* 6, 217–220 (1984)

Jordan EG, McGovern JH: The quantitative relationship of the fibrillar centers and other nucleolar components to changes in growth conditions, serum deprivation and low doses of actinomycin D in cultured diploid human fibroblasts (strain MRC-5). *J Cell Sci* 52, 373–389 (1981)

Leader DJ, Clark GP, Watters J, Beven AF, Shaw PJ, Brown JWS: Clusters of multiple different small nucleolar RNA genes in plants are expressed as and processed from polycistronic pre-snoRNAs. *EMBO J* 16, 5742–5751 (1997)

Leitch AR, Mosgoller W, Shi M, Heslop-Harrison JS: Different patterns of rDNA organization at interphase in nuclei of wheat and rye. *J Cell Sci* 101, 751–757 (1992)

Martin M, Medina FJ: A Drosophila anti-RNA polymerase II antibody recognizes a plant nucleolar antigen, RNA polymerase I, which is mostly localized in fibrillar centers. *J Cell Sci* 100, 99–108 (1992)

Motte PM, Loppes R, Menager M, Deltour R: Three-dimensional electron microscopy of ribosomal chromatin in two higher plants: A cytochemical, immunocytochemical, in situ hybridization approach. *J Histochem Cytochem* 39, 1495–1506 (1991)

Risueno MC, Medina FJ, Moreno Diaz dela Espina S: Nucleolar fibrillar centeres in plant meristematic cells: Ultrastructure, cytochemistry and autoradiography. *J Cell Sci* 58, 313–329 (1982)

Sano Y, Sano R: Variation of the intergenic spacer region of ribosomal DNA in cultivated and wild rice species *Genome* 33, 209–218 (1990)

Sato S: Three-dimensional architecture of the higher plant nucleolonema disclosed on serial ultrathin sections. *Biol Cell* 75, 225–233 (1992)

Sato S, Myoraku A: Three-dimensional organization of nucleolar DNA in the higher plant nucleonema studied by immunoelectron microscopy. *Micron* 25, 431–437 (1994)

Sato M, Tamochi R, Suzuki T and Goto M: Effect of detector geometries on SEM images. *Hitachi Review* 43, 191–194 (1994)

Scheer U, Rose KM: Localization of RNA polymerase-I in interphase cells and mitotic chromosomes by light and electron microscopic immnocytochemistry. *Proc Natl Acad Sci USA* 81, 1431–1435 (1984)

Shaw PJ, Jordan EG: The nucleolus. *Annu Rev Cell Dev Biol* 11, 93–121 (1995)

Shaw PJ, Highett MI, Beven AF, Jordan EG: The nucleolar architecture of polymerase I transcription and processing. *EMBO J* 12, 2896–2906 (1995)

Stahl A, Wachtler F, Hartung M, Devictor M, Schofer C, Mosgoller W, Lanversin A, Fouet C, Schwarzacher HG: Nucleoli, nucleolar chromosomes and ribosomal genes in the human spermatocyte. *Chromosoma* 101, 231–244 (1991)

Suzaki E, Kataoka K: Lectin cytochemistry in the gastrointestinal tract with special reference to glycosylation in the Golgi apparatus of Brunner's gland cells. *J Histochem* 40, 379–385 (1992)

Thiry M, Thiry-Blaise L: In situ hybridization at the electron-microscope level: An improved method for precise localization of ribosomal DNA and RNA. *Eur J Cell Biol* 50, 235–243 (1989)

Yano H, Sato S: Ultrastructural localization of transcription sites, DNA, and RNA reveals a concentric arrangement of structural and functional domains in plant nucleonema. *Protoplasma* 214, 129–140 (2000)

Wachtler F, Stahl A: The nucleolus: a structural and functional interpretation. *Micron Microsc Acta* 24, 473–505 (1993)